

The Compton Mirror in NGC 4151

Juri Poutanen^{1,2}, Marek Sikora^{1,3}, Mitchell C. Begelman⁴, and Paweł Magdziarz⁵

ABSTRACT

We show that the sharp cutoff in the hard X-ray spectrum of NGC 4151, unusual for Seyfert 1 galaxies, can be reconciled with the average Seyfert 1 spectrum if we assume that the central source is completely hidden from our line of sight by the thick part of the accretion disk or by the broad emission line clouds. The observed X-ray radiation is produced by scattering of the Seyfert 1-type spectrum in the higher, cooler parts of the accretion disk corona, or in a wind. A sharp cutoff appears as a result of the Compton recoil effect. This model naturally explains a discrepancy regarding the inclination of the central source, inferred to be low (face-on) from observations of the iron $K\alpha$ emission line, but inferred to be high on the basis of optical and UV observations.

Subject headings: accretion, accretion disks – galaxies: individual (NGC 4151) – galaxies: Seyfert – gamma rays: theory – radiation mechanisms: thermal – X-rays: galaxies

1. Introduction and Conclusions

The brightest Seyfert galaxy in X-rays, NGC 4151, has a significantly different spectrum from the average Seyfert 1 spectrum. The average hard X-ray Seyfert 1 spectrum is well described by a power-law with exponential cutoff at energy, $E_c \sim 300 - 1000$ keV, and a Compton reflection component. The spectrum of NGC 4151 has a much sharper decline in hard X-rays and no clear signature of a reflection component. While the X-ray spectra of both an average Seyfert 1 and NGC 4151 can be well described by models invoking thermal Comptonization of the soft radiation from the accretion disk in a hot corona, the corona in NGC 4151 is required to be much thicker (Thomson optical depth $\tau_T \sim 2$) and much cooler ($T_e \sim 40 - 50$ keV) than the corona of Seyfert 1s, for which $\tau_T \sim 0.2 - 0.3$ and $T_e \sim 200 - 300$ keV (Zdziarski et al. 1995, 1996).

¹Stockholm Observatory, S-133 36 Saltsjöbaden, Sweden; juri@astro.su.se

²Institute for Theoretical Physics, University of California, Santa Barbara, CA 93106-4030

³Nicolaus Copernicus Astronomical Center, Bartycka 18, 00-716 Warsaw, Poland; sikora@camk.edu.pl

⁴JILA, University of Colorado, Boulder, CO 80309; mitch@jila.colorado.edu; also Department of Astrophysical, Planetary, and Atmospheric Sciences, University of Colorado, Boulder

⁵Astronomical Observatory, Jagiellonian University, Orla 171, 30-244 Cracow, Poland; pavel@oa.uj.edu.pl

In this Letter we argue that the intrinsic spectrum of NGC 4151 does not differ from that of Seyfert 1s, if we assume that the direct component is hidden from our line of sight by the outer parts of the accretion disk or by the broad emission line region (BLR) close to the central source (Jourdain & Roques 1995) and that the observed X-ray radiation is due to scattering in the higher, cooler parts of the accretion disk corona or in a wind. The observed Compton-scattered component has much sharper cutoff than the intrinsic spectrum due to the Compton recoil effect. We show also that the primary X-ray spectrum of NGC 4151 is consistent with thermal Comptonization in active regions in the vicinity of a relatively cold accretion disk and that optical depths and temperatures of the hot plasma do not differ from those of Seyfert 1s. Non-thermal models cannot be ruled out, as a strong annihilation line will be smeared out by scattering. The scattered component is further filtered through a complex absorber. The absorption clearly visible in the X-ray spectrum of NGC 4151 can be provided by the extended “atmosphere” of the accretion disk or BLR.

The edge-on orientation of the NGC 4151 nucleus is strongly supported by the biconical geometry of the [OIII] $\lambda 5007$ region (Evans et al. 1993; Pedlar et al. 1993). The observed geometry requires the observer to be located outside the cone of UV radiation which photoionizes the oxygen. Recent observations of the profile of the iron $K\alpha$ line, showing an extended luminous red wing and a sharp cutoff on the blue side, suggest an accretion disk viewed face-on (Yaqoob et al. 1995). This can be reconciled with the edge-on geometry deduced from the [OIII] $\lambda 5007$ image, if the central source is observed through the radiation scattered by electrons in an extended corona or wind.

Finally, after correcting the UV and X-ray luminosities for dilution due to scattering, one also finds that NGC 4151 has luminosity ratios, L_{UV}/L_{OIII} and L_X/L_{OIII} , typical of Seyfert 1s (Mulchaey et al. 1994).

2. Scattering Model

The scattering region is assumed to be situated along the axis of the accretion disk in the form of a cone (we call it the “scattering cone”). In order to avoid additional parameters, we assume that the radiation coming from the central source is scattered to our line of sight at a given angle. This angle was fixed at $i = 65^\circ$, which is the best estimate obtained from optical and radio observations (Evans et al. 1993; Pedlar et al. 1993).

For an arbitrary intrinsic radiation spectrum described by the photon number density, $f_{\text{intr}}(x)$, the Compton scattered component can be found using the Klein-Nishina formula:

$$f_{\text{scat}}(x, i) \propto \tau_{\text{sc}} \left[1 + \mu^2 + x x_1 (1 - \mu)^2 \right] f_{\text{intr}}(x_1), \quad (1)$$

where $x = h\nu/m_e c^2$ is the dimensionless photon energy, $\mu = \cos i$, $x_1 = x/[1 - x(1 - \mu)]$, and τ_{sc} is the Thomson optical depth of the scattering material. Here we assume that the electron temperature is much smaller than $m_e c^2$ and that the bulk velocity in the scattering region is

small compared with the speed of light. Under such assumptions the scatterer can be treated as static and the Compton scattering cross-section for cold electrons can be applied. Then, for small photon energies ($x \lesssim 0.1$) the shape of the spectrum remains the same, but at higher energies, the cutoff appears much sharper than in the intrinsic spectrum due to the Compton recoil.

3. Spectral Fitting

We fit nearly simultaneous observations of NGC 4151 by *ROSAT*, *Ginga*, and OSSE in 1991 June/July (Obs 1), and *ASCA* and OSSE in 1993 May (Obs 2). Description of the broad-band data can be found in Zdziarski et al. (1996). We used XSPEC v. 8.5 (Shafer, Haberl, & Arnaud 1991) to fit the data.

3.1. Exponentially Cutoff Power-Law with Compton Reflection

We apply the scattering model described in § 2, where the intrinsic spectrum is represented as a sum of an exponentially cut-off power-law and a Compton reflected component. This type of spectrum gives a good description of the spectra of Seyfert 1 galaxies (Nandra & Pounds 1994; Zdziarski et al. 1995). We use the Compton reflection model of Magdziarz & Zdziarski (1995). The parameters of the model are spectral energy index, α , cutoff energy, E_c , and the amount of reflection, R . For an isotropic source illuminating a flat reflecting slab, $R = 1$ is expected. The iron line component is modeled by the “disk-line” model of Fabian et al. (1989). The inner and outer radii of the accretion disk, r_i and r_o , are fixed at 6 and 1000 Schwarzschild radii, r_G , respectively. The line energy, E_{Fe} , and the emissivity index, q (characterizing the line emissivity as $\propto r^{-q}$), are allowed to vary. The intrinsic spectrum corresponds to the inclination $i = 0^\circ$. The scattered component is further transmitted through a complex absorber, which we approximate by a conventional dual absorber model with column densities N_{H}^1 , covering the whole source, and N_{H}^2 , covering a fraction C_F of the source (Weaver et al. 1994). In our case, by the source we mean the scattered component. We use the abundances from Morrison & McCammon (1983). As discussed in Warwick, Done, & Smith (1995) and Zdziarski et al. (1996), the data below 1 keV show a separate soft component which we model by a power-law with exponential cutoff at 100 keV. An additional neutral absorber with column density, $N_{\text{H}}^{\text{soft}}$, exceeding the Galactic value of $2.1 \cdot 10^{20} \text{ cm}^{-2}$ (Stark et al. 1992) covers the whole source.

In spectral fitting we use only one reflection component with $i = 0^\circ$, which corresponds to the radiation reflected from the accretion disk and scattered in the scattering cone. However, we expect the existence of another component arising, e.g., from the far wall of the obscuring medium if the latter has the form of an opaque torus (Ghisellini, Haardt, & Matt 1994; Krolik, Madau, & Źycki 1994). It is impossible to distinguish between these reflection components, and it is also quite difficult to separate reflected and scattered radiation at high energies as both have a sharp

cutoff due to Compton recoil.

The *Ginga* data (Obs 1) provide good constraints on the amount of reflection, giving a best fit value of $R = 0.30 \pm 0.13$, which is less than is typically found in Seyfert 1s. In § 4 we give possible explanations for the weak reflection in NGC 4151. The *ASCA* data (Obs 2) do not constrain the amount of reflection, and the inferred values of R , α , and E_c are strongly correlated. The data do not require a reflection component, but its presence cannot be ruled out. For Obs 2, we fix R at the best fit value for Obs 1. The best fit parameters are given in Table 1.

The cutoff of the intrinsic spectrum ($E_c \sim 200 - 500$ keV) appears at a much higher energy than in the models without scattering ($E_c \sim 80 - 140$ keV, Zdziarski et al. 1996), and is in very good agreement with the cutoff of the average Seyfert 1 spectrum ($E_c = 560_{-240}^{+840}$ keV) and the cutoff of the average spectrum of all Seyfert galaxies ($E_c = 320_{-70}^{+110}$ keV, see Zdziarski et al. 1995). Both observed spectra of NGC 4151 are harder than the average Seyfert 1 spectrum. For Obs 1, the power-law index, α , of 0.7 (cf. Table 1) is inside the range of observed power-law indices of Seyfert 1s (Nandra & Pounds 1994), while $\alpha \sim 0.5$ in Obs 2 is much flatter.

3.2. Two-Phase Disk-Corona Model

As it is already mentioned, spectra of Seyfert galaxies can be well described by thermal Comptonization models (Haardt & Maraschi 1993; Stern et al. 1995). In two-phase model for an accretion disk-corona, soft (black body) radiation from the accretion disk gets Comptonized by hot thermal electron (-positron) coronal plasma. We consider two geometries of the corona: plane-parallel slab and localized active region in the form of a pill-box (cylinder, with height-to-radius ratio equal to unity). The method of Poutanen & Svensson (1996) to compute Comptonized spectra taking reflection from the cold disk into account is applied. The spectrum scattered by cold matter in the outer part of the corona is found from equation (1) where an intrinsic spectrum is the face-on spectrum of the accretion disk-corona system. The parameters of the model are temperature of the cold disk, T_{bb} , coronal electron temperature, T_e , and the optical depth of the corona, τ_T . We fix $T_{bb} = 10$ eV, because this parameter is purely constrained by the data. The same models for the iron line, absorber, and soft component as in § 3.1 are used.

For the slab corona, the best fit parameters $(T_e, \tau_T) = (210 \text{ keV}, 0.24)$ and $(218 \text{ keV}, 0.30)$ for Obs 1 and 2, respectively, do not satisfy the energy balance between hot and cold phases (Haardt & Maraschi 1993; Stern et al. 1995). The pill-box-corona model gives $T_e = 210$ keV and $\tau_T = 0.54$ for Obs 1 (see Table 1). This is consistent with the situation where all energy is dissipated in an active region detached from the cold disk at approximately a height equal to half of its radius. In this condition, the X-ray source is photon-starved, and the covering factor (fraction of the reprocessed radiation returning to the active region) is ~ 0.4 (see Stern et al. 1995; Zdziarski et al. 1996). The best fit to Obs 2 gives $T_e = 290$ keV and $\tau_T = 0.49$. The energy balance requires dissipation of energy in an active region detached from the cold disk at a height comparable to its radius, implying a covering factor ~ 0.15 . For pure pair corona, the compactness parameter, l

(for definition, see, e.g., Stern et al. 1995), is about 100 in both cases. The corresponding model spectra are shown in Figure 1.

Parameter	Obs 1		Obs 2	
	CPLR	PBC	CPLR	PBC
E_c or T_e (keV)	320_{-60}^{+170}	210_{-30}^{+10}	280_{-80}^{+140}	290_{-120}^{+110}
α	$0.67_{-0.05}^{+0.07}$...	$0.50_{-0.08}^{+0.07}$...
R	$0.30_{-0.13}^{+0.13}$...	0.30^f	...
τ_T	...	$0.54_{-0.07}^{+0.11}$...	$0.49_{-0.21}^{+0.31}$
N_H^1 (10^{22} cm $^{-2}$)	$4.8_{-1.0}^{+0.9}$	$4.8_{-1.1}^{+1.0}$	$4.1_{-0.9}^{+0.8}$	$4.1_{-0.5}^{+0.5}$
N_H^2 (10^{22} cm $^{-2}$)	$4.7_{-0.8}^{+1.0}$	$5.4_{-0.8}^{+1.1}$	$12.9_{-2.5}^{+3.6}$	$13.8_{-1.6}^{+2.0}$
C_F	$0.76_{-0.16}^{+0.17}$	$0.75_{-0.21}^{+0.14}$	$0.71_{-0.07}^{+0.07}$	$0.71_{-0.07}^{+0.06}$
E_{Fe} (keV)	$6.68_{-0.25}^{+0.23}$	$6.74_{-0.24}^{+0.40}$	$6.46_{-0.06}^{+0.05}$	$6.46_{-0.04}^{+0.05}$
q	$3.3_{-0.5}^{+0.6}$	$3.1_{-0.5}^{+0.9}$	$2.2_{-0.4}^{+0.3}$	$2.2_{-0.4}^{+0.2}$
EW (eV)	197_{-38}^{+16}	239_{-35}^{+35}	279_{-93}^{+93}	277_{-79}^{+74}
α_{soft}	$1.75_{-0.09}^{+0.15}$	$1.75_{-0.09}^{+0.15}$	$1.33_{-0.24}^{+0.70}$	$1.29_{-0.15}^{+0.68}$
N_H^{soft} (10^{22} cm $^{-2}$)	$0.03_{-0.00}^{+0.01}$	$0.03_{-0.00}^{+0.01}$	$0.03_{-0.01}^{+0.08}$	$0.03_{-0.01}^{+0.07}$
$\chi^2/d.o.f.$	114/100	110/101	311/309	318/309

Table 1: Best Fit Parameters for 1991 June/July (Obs 1) and 1993 May (Obs 2) Observations of NGC 4151

Note. — CPLR - exponentially cutoff power-law plus Compton reflection. Reflection model of Magdziarz & Zdziarski (1995) was used.

PBC - pill-box-corona model by Poutanen & Svensson (1996).

All errors are for $\Delta\chi^2 = 2.7$.

4. Discussion

Observations of optical emission lines from the narrow line region in NGC 4151 indicate that the gas there is illuminated by an ionizing continuum stronger than the continuum observed from Earth by a factor 13 (Penston et al. 1990). NGC 4151 also has relatively small luminosity ratios L_{UV}/L_{OIII} and L_X/L_{OIII} , compared to Seyfert 1 galaxies (Mulchaey et al. 1994). This suggests that intrinsic UV and X-ray luminosities are underestimated by at least a factor of ten. Observations of the “ionizing cone” (Evans et al. 1993) clearly show the anisotropy of UV radiation in NGC 4151. Our models, in which the central source is completely covered by optically thick matter and the only radiation we see is the radiation scattered in the cone, easily explain these properties.

Let us assume that the inner edge of the scattering cone is $r_0 = 30 r_G = 3 \cdot 10^{14}$ cm (for a black hole mass $5 \cdot 10^7 M_\odot$, Ulrich et al. 1984, Clavel et al. 1987). This is supported by the X-ray variability time-scale (Yaqoob & Warwick 1991). The scatterer can be produced by a wind from

the accretion disk. It can be highly ionized matter of normal composition or pure pair plasma. From observations we cannot distinguish between these alternatives. The ionization parameter, $\xi = L/r^2 n_e$, is of order 10^7 at $r \sim 10^{15}$ cm. Thus, highly ionized matter can scatter radiation out from the scattering cone without imprinting a spectral line signature on it. Assuming that the electron density decreases along the cone as $n_e = n_e^0(r/r_0)^{-2}$ and that $\tau_{\text{sc}} \sim 0.2$, we can estimate the electron density at the inner edge of the cone, $n_e^0 = 10^9$ cm $^{-3}$. The velocity of the wind would be approximately $v \sim 0.1c$, which is the terminal velocity of a particle if radiation and gravitational forces are of the same order and the particle is at rest at $10 r_G$ from the center. The rate of pair production to feed the wind, \dot{n}_{pair} , should be about 10^{48} s $^{-1}$. Assuming $L_X = 3 \cdot 10^{44}$ erg s $^{-1}$ and a pair yield of 1% (the fraction of luminosity converted into rest mass of pairs; see, e.g., Maciołek-Niedźwiecki, Zdziarski, & Coppi 1995), we get a pair production rate $\dot{n}_{\text{pair}} \sim 2 \cdot 10^{48}$ s $^{-1}$. This shows that a pair wind is consistent with both the inferred intrinsic X-ray flux and the required scattering optical depth. Pairs are expected to have a Compton temperature of order $10^7 - 10^8$ K.

One of the most intriguing properties of NGC 4151 is that different column densities of absorbing material are inferred from observations in UV ($N_{\text{H}} \sim 10^{19} - 10^{21}$ cm $^{-2}$, Kriss et al. 1992) and in X-rays ($N_{\text{H}} \sim 10^{22} - 10^{23}$ cm $^{-2}$, Yaqoob et al. 1993). Coexistence of warm and cold absorbers can explain this discrepancy (Evans et al. 1993; Warwick et al. 1995). The observed UV and X-rays can be scattered at similar distances from the central source, consistent with the observed temporal correlations between the flux in these two frequency bands (Perola et al. 1986; Edelson et al. 1996).

The *Ginga* data show that the reflection component is rather weak in NGC 4151 (see § 3.1, and Maisack & Yaqoob 1991). Gondek et al. (1996) found that the average Seyfert 1 also exhibits a deficit of reflection, having $R = 0.67^{+0.13}_{-0.12}$. If the underlying continuum is produced by Comptonization, then the spectral break appears at energies corresponding to the maximum of the second scattering order and is caused by anisotropy of the soft photons coming from the accretion disk (Stern et al. 1995). For a source compactness $l \sim 100$, the *anisotropy break* lies in the 2 – 10 keV energy range (see Fig. 3 in Stern et al. 1995, and dotted curves in our Fig. 1). The overall spectrum, being the sum of the Compton reflected spectrum and a broken power-law, is almost a perfect power-law in the 2 – 20 keV band. This explains a deficit of reflection in Seyfert 1s. If the intrinsic face-on spectrum has an amount of reflection (from the accretion disk) $R \sim 0.6 - 0.7$, then the scattered radiation is expected to have $R \sim 0.3 - 0.4$ due to the angular average.

In the case of a torus-like geometry of obscuring matter, we can expect also some contribution due to reflection from the side of the torus opposite to the observer or from the outer part of the accretion disk. The actual fraction of the reflected radiation depends on the angular distribution of the intrinsic radiation, the exact geometry of the absorbing (reflecting) medium, clumpiness of the matter, etc. It can be about 15% for a torus geometry, assuming that optically thick material just covers the central source and the inclination angle is 65°, and less than 4% if the surface of the accretion disk is cone-like with a constant opening angle $\sim 120^\circ$. This would correspond to

the amount of reflection $R \sim 0.1 - 0.4$ assuming $\tau_{\text{sc}} \sim 0.3$ (note that in our model the intrinsic spectrum corresponds to $i = 0^\circ$, and R is normalized to the scattered component). Since the data suggest $R < 0.5$, we conclude that either geometrical effects reduce the amount of reflection from the torus, the central source is anisotropic, and/or the reflecting (obscuring) matter is clumpy.

The equivalent width of the iron line ($EW \sim 200 - 300$ eV) is in agreement with the predictions of the two-phase disk-corona models (Poutanen, Nagendra, & Svensson 1996). It is significantly higher than expected from the irradiation of cold matter by isotropic X-ray radiation having a power-law shape (George & Fabian 1991), due to the anisotropy of the Comptonized radiation. While the inclination of the central torus-like region is suggested to be high based on the Balmer line reverberation mapping (Maoz et al. 1991), recent observations of the iron line profile (Yaqoob et al. 1995) strongly suggest that we see the accretion disk almost face-on. This discrepancy has a simple explanation in the scattering model, as we see the central source via a “mirror” situated above the disk.

The intrinsic spectrum of NGC 4151 can be produced by thermal Comptonization in localized active regions above a cold accretion disk. The compactness parameter is high, and therefore a significant fraction of hot plasma is expected to be in the form of electron-positron pairs. A pair model can also naturally explain the origin of the scattering material, as a pair wind. Despite the fact that a thermal model gives an excellent fit to observations, the presence of non-thermal processes cannot be ruled out. While non-thermal models predict a large flux at $E \sim 500$ keV due to pair annihilation, this flux is significantly diminished due to scattering by cold matter.

An increasing fraction of the central source radiation is transmitted through the obscuring matter due to the Klein-Nishina decline of the Compton scattering cross-section at higher energies. Upper limits on the γ -ray flux at $E \sim 400$ keV (see Fig. 1) provide some constraints on the Thomson optical thickness of the obscuring matter, τ_{obsc} . Assuming that the intrinsic flux is ten times larger than the observed one, we get $\tau_{\text{obsc}} \gtrsim 6$.

A crucial test for the scattering model will be future observations of polarization in X-rays with the Spectrum-X- γ satellite (1997). The scattering model predicts a polarization of about 20-30% perpendicular to the axis of the scattering cone.

The authors thank Boris Stern and Roland Svensson for valuable discussions. This research was supported by NASA grants NAG5-2026, and NAGW-3016; NSF grants AST91-20599, INT90-17207, and PHY94-07194; the Polish KBN grants 2P03D01008 and 2P03D01410; and by grants from the Swedish Natural Science Research Council.

REFERENCES

Clavel, J., et al. 1987, *ApJ*, 321, 251

Edelson, R. A., et al. 1996, *ApJ*, submitted

Evans, I. N., Tsvetanov, Z., Kriss, G. A., Ford, H. C., Caganoff, S., & Koratkar, A. P. 1993, *ApJ*, 417, 82

Fabian, A. C., Rees, M. J., Stella, L., & White, N. E. 1989, *MNRAS*, 238, 729

George, I. M., & Fabian, A. C. 1991, *MNRAS*, 249, 352

Ghisellini, G., Haardt, F., & Matt, G. 1994, *MNRAS*, 267, 743

Gondek, D., Zdziarski, A. A., Johnson, W. N., George, I. M., McNaron-Brown, K., & Gruber, D. E. 1996, *MNRAS*, submitted

Haardt, F., & Maraschi, L. 1993, *ApJ*, 413, 507

Jourdain, E., & Roques, J. P. 1995, *ApJ*, 440, 128

Kriss, G. A., et al. 1992, *ApJ*, 392, 485

Krolik, J. H., Madau, P., & Źycki, P. T. 1994, *ApJ*, 420, L57

Maciołek-Niedźwiecki, A., Zdziarski, A. A., & Coppi, P. S. 1995, *MNRAS*, 276, 273

Magdziarz, P., & Zdziarski, A. A. 1995, *MNRAS*, 273, 837

Maisack, M., & Yaqoob, T. 1991, *A&A*, 249, 25

Maoz, S., et al. 1991, *ApJ*, 367, 493

Morrison, R., & McCammon, D. 1983, *ApJ*, 270, 119

Mulchaey, J. S., et al. 1994, *ApJ*, 436, 586

Nandra, K., & Pounds, K. A. 1994, *MNRAS*, 268, 405

Pedlar, A., Kukula, M. J., Longley, D. P. T., Muxlow, T. W. B., Axon, D. J., Baum, S., O'Dea, C., & Unger, S. W. 1993, *MNRAS*, 263, 471

Penston, M. V., et al. 1990, *A&A*, 236, 53

Perola, G. C., et al. 1986, *ApJ*, 306, 508

Poutanen, J., & Svensson, R. 1996, *ApJ*, in press

Poutanen, J., Nagendra, K.N., & Svensson, R. 1996, *A&AS*, submitted

Shafer, R. A., Haberl, F., & Arnaud, K. A. 1991, XSPEC: An X-ray Spectral Fitting Package. ESA TM-09, ESA, Paris

Stark, A. A., Gammie, C. F., Wilson, R. W., Bally, J., Linke, R. A., Heiles, C., Hurwitz, M. 1992, *ApJS*, 79, 77

Stern, B. E., Poutanen, J., Svensson, R., Sikora, M., & Begelman, M. C. 1995, *ApJ*, 449, L13

Ulrich, M.-H., et al. 1984, *MNRAS*, 206, 221

Weaver, K. A., Yaqoob, T., Holt, S. S., Mushotzky, R. F., Matsuoka, M., & Yamauchi, M. 1994, *ApJ*, 436, L27

Warwick, R. S., Done, C., & Smith, D. A. 1995, *MNRAS*, 275, 1003

Yaqoob, T., & Warwick, R. S. 1991, *MNRAS*, 248, 773

Yaqoob, T., Warwick, R. S., Makino, F., Otani, C., Sokoloski, J. L., Bond, I. A., & Yamauchi, M. 1993, *MNRAS*, 262, 435

Yaqoob, T., Edelson, R., Weaver, K. A., Warwick, R. S., Mushotzky, R. F., Serlemitsos, P. J., & Holt, S. S. 1995, *ApJ*, 453, L81

Zdziarski, A. A., Johnson, W. N., Done, C., Smith, D., & McNaron-Brown, K. 1995, *ApJ*, 438, L63

Zdziarski, A. A., Johnson W. N., & Magdziarz, P. 1996, *MNRAS*, submitted

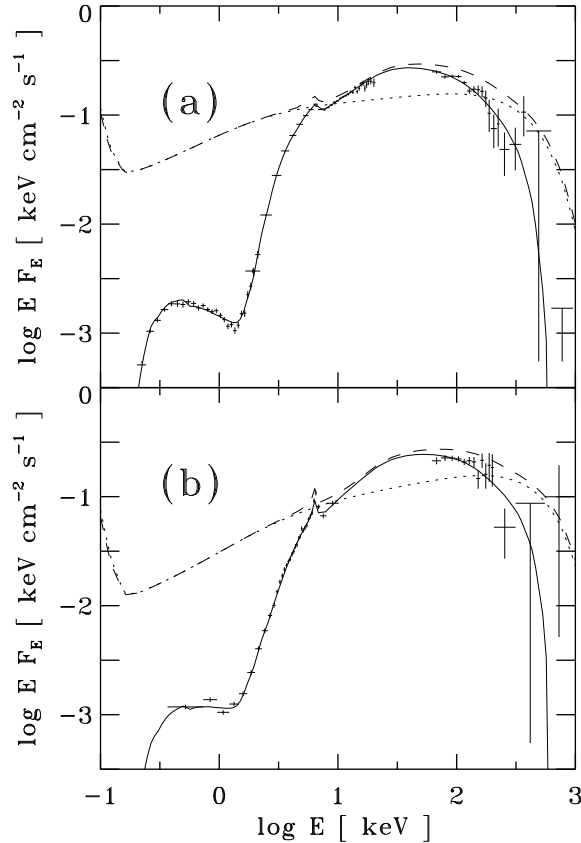


Fig. 1.— (a) Spectrum of NGC 4151 observed in June/July 1991 by *ROSAT*, *Ginga*, and OSSE. *Solid curve* represents the best fit model spectrum for pill-box-corona model (PBC, see Table 1). *Dashed curve* represents the intrinsic spectrum of the disk-corona system which is seen by the scattering medium (normalized to the scattered component). *Dotted curve* represents the underlying Comptonized spectrum (without reflection from the cold disk), which can be approximated by a broken power-law. The upper limits are 2σ . (b) Same as (a), but for observations in May 1993 by *ASCA* and OSSE.